Journal of Medicinal Chemistry

ARTICLE

pubs.acs.org/jmc

# Comparison of the Reactivity of Antimalarial 1,2,4,5-Tetraoxanes with 1,2,4-Trioxolanes in the Presence of Ferrous Iron Salts, Heme, and Ferrous Iron Salts/Phosphatidylcholine

Fatima Bousejra-El Garah,*[,†] Michael He-Long Wong,[‡] Richard K. Amewu,[†] Sant Muangnoicharoen,[§] James L. Maggs,[‡] Jean-Luc Stigliani,[∥] B. Kevin Park,[‡] James Chadwick,[†] Stephen A. Ward,[§] and Paul M. O'Neill*[,†]

[†]Department of Chemistry, University of Liverpool, Liverpool L69 7ZD, U.K.

[‡]MRC Centre for Drug Safety Science, Department of Molecular and Clinical Pharmacology, University of Liverpool, Sherrington Building, Liverpool L69 3GE, U.K.

[§]Liverpool School of Tropical Medicine, Pembroke Place, Liverpool L3 5QA, U.K.

[∥]Laboratoire de Chimie de Coordination, Université de Toulouse, 31077 Toulouse Cedex 4, France

Supporting Information

**ABSTRACT:**

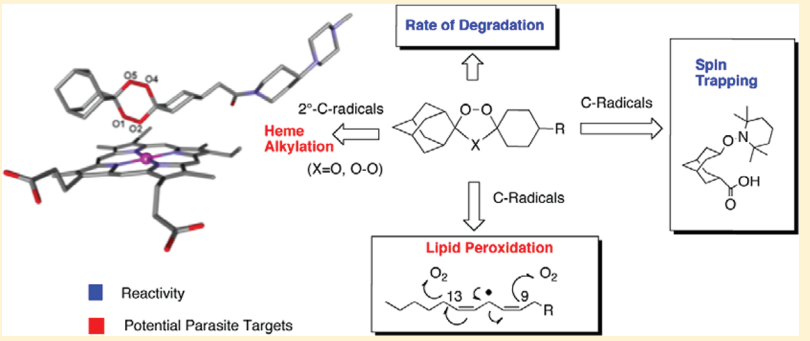


Dispiro-1,2,4,5-tetraoxanes and 1,2,4-trioxolanes represent attractive classes of synthetic antimalarial peroxides due to their structural simplicity, good stability, and impressive antimalarial activity. We investigated the reactivity of a series of potent amide functionalized tetraoxanes with Fe(II)gluconate, $FeSO_4$, $FeSO_4$/TEMPO, $FeSO_4$/phosphatidylcholine, and heme to gain knowledge of their potential mechanism of bioactivation and to compare the results with the corresponding 1,2,4-trioxolanes. Spin-trapping experiments demonstrate that Fe(II)-mediated peroxide activation of tetraoxanes produces primary and secondary C-radical intermediates. Reaction of tetraoxanes and trioxolanes with phosphatidylcholine, a predominant unsaturated lipid present in the parasite digestive vacuole membrane, under Fenton reaction conditions showed that both endoperoxides share a common reactivity in terms of phospholipid oxidation that differs with that of artemisinin. Significantly, when tetraoxanes undergo bioactivation in the presence of heme, only the secondary C-centered radical is observed, which smoothly produces regioisomeric drug derived-heme adducts. The ability of these tetraoxanes to alkylate the porphyrin ring was also confirmed with $Fe^{II}$TPP and $Mn^{II}$TPP, and docking studies were performed to rationalize the regioselectivity observed in the alkylation process. The efficient process of heme alkylation and extensive lipid peroxidation observed here may play a role in the mechanism of action of these two important classes of synthetic endoperoxide antimalarial.

## INTRODUCTION

According to the World Health Organization, more than one million people die of malaria every year in Africa, countries where children and pregnant women are especially at risk.[1] The spread of chloroquine and sulfadoxine-pyrimethamine resistance have been implicated in the re-emergence of malaria in areas where the disease had been eradicated. In order to control the burden of malaria, artemisinin-based combination therapies are now recommended as a first-line treatment in many endemic regions.[2]

Artemisinin (Figure 1), a sesquiterpene lactone extracted from the Chinese herb *Artemisia annua*, is highly active against both chloroquine sensitive- and resistant-strains of *Plasmodium falciparum*.[3] It is known that the key pharmacophore of artemisinin is the endoperoxide containing 1,2,4-trioxane unit.[3] It is also well established that iron(II) salts reductively activate the

**Received:** September 7, 2010
**Published:** September 05, 2011





dx.doi.org/10.1021/jm200768h | *J. Med. Chem.* 2011, 54, 6443–6455

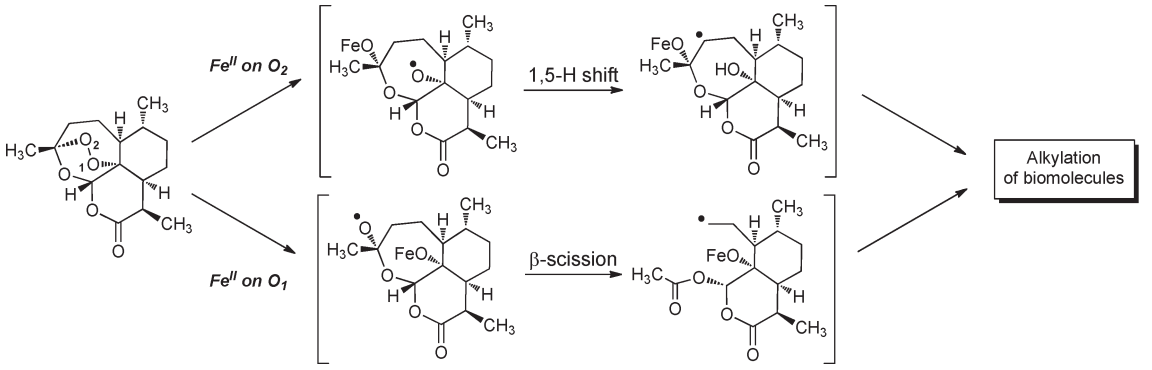


**Figure 1.** Fe(II)-mediated activation of artemisinin.

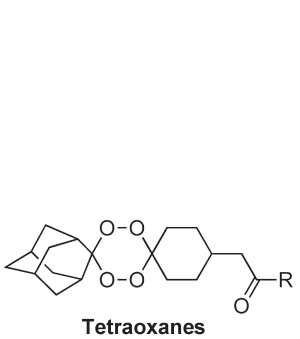


| Compound | R | $IC_{50}$ *vs.* 3D7 (nM) |
|---|---|---|
| **1** | $OCH_2CH_3$ | 10.0 |
| **2** | 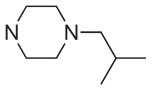 | 1.4 |
| **3** | 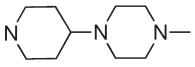 | 0.4 |
| **4** |  | 5.2 |
| **5** |  | 2.3 |
| **6** | 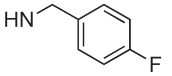 | 3.0 |

**Figure 2.** Structures of antimalarial tetraoxanes **1**−**6** and their activities against 3D7 *Plasmodium falciparum*.

peroxide bond of artemisinin leading to the formation of a pair of oxyl radical intermediates that rapidly rearrange via either a 1,5 H-shift or $\beta$-scission to produce the more stable carbon-centered radicals.[4−6] These alkyl radicals can be readily formed in vivo by the reaction of artemisinin with iron(II)-heme,[7,8] the most abundant source of iron in *Plasmodia*.[7,9] It is proposed that these reactive C-radicals interact with cellular components such as heme and parasite proteins[10] resulting in the death of the parasite (Figure 1). One such protein is PfATP6, the sarco/endoplasmic reticulum calcium ATPase of *P. falciparum*, reported by Krishna and us to be inhibited by artemisinin in *Xenopus laevis* oocytes.[11] However, recent studies on purified PfATP6[12] and modeling calculations[13] have questioned the role of PfATP6 as a drug target. As noted above, heme has also been proposed to play a role in the mechanism of action of endoperoxides, and supportive in vivo evidence was provided in a study where heme-artemisinin adducts were detected in infected mice treated with artemisinin. Inspite of this work, the mechanism of action of artemisinin and synthetic endoperoxides remains controversial, and very recently, a non iron-mediated mechanism of bioactivation has been proposed by Haynes and Monti.[14,15] While these studies provide an attractive alternative mechanism of activation, additional biological support for this proposal is urgently needed.

Work by the Vennerstrom group in the early 1990s showed that dispiro-tetraoxanes possess high in vitro antimalarial activity.[16] More recently, we have designed and prepared simple, achiral, and highly potent dispiro-tetraoxanes that incorporate the adamantyl group, known to bring stability to the endoperoxide motif.[17,18] From a library of over 200 tetraoxanes, **3** (RKA182) (Figure 2) has been selected as a candidate for full formal preclinical development. Compound **3** has outstanding in vitro and in vivo activity against *P. falciparum* and shows improved pharmacokinetic characteristics compared to those of other peroxide drugs.[19]

The first aim of the present study was to investigate the radical pathway after reductive activation of highly potent tetraoxanes (selected from **2**−**6**, vide infra) with inorganic iron(II). Second, we set out to investigate whether the oxidative degradation of phospholipids, recently reported for water-soluble tetraoxanes,[20] was observed with adamantane functionalized tetraoxanes and their corresponding trioxolane analogues. In our model studies, we employed phosphatidylcholine (PC) on the basis of research by Tilley that clearly demonstrates that PC is a major constituent of the food vacuole cell membranes of *P. falciparum*.[21] Our third aim was to explore the reactivity of 1,2,4,5-tetraoxanes with heme for comparison with that of 1,2,4-trixolanes and to rationalize differences in reactivity with inorganic iron sources. While these studies may be fundamental to the mechanism of action, the importance of understanding the ferrous ion reactivity of these systems is also key to producing molecules that provide good exposures in malaria infected patients. As seen recently with **15** (OZ277), degradation in the plasma of infected patients, by iron


dx.doi.org/10.1021/jm200768h |*J. Med. Chem.* 2011, 54, 6443–6455

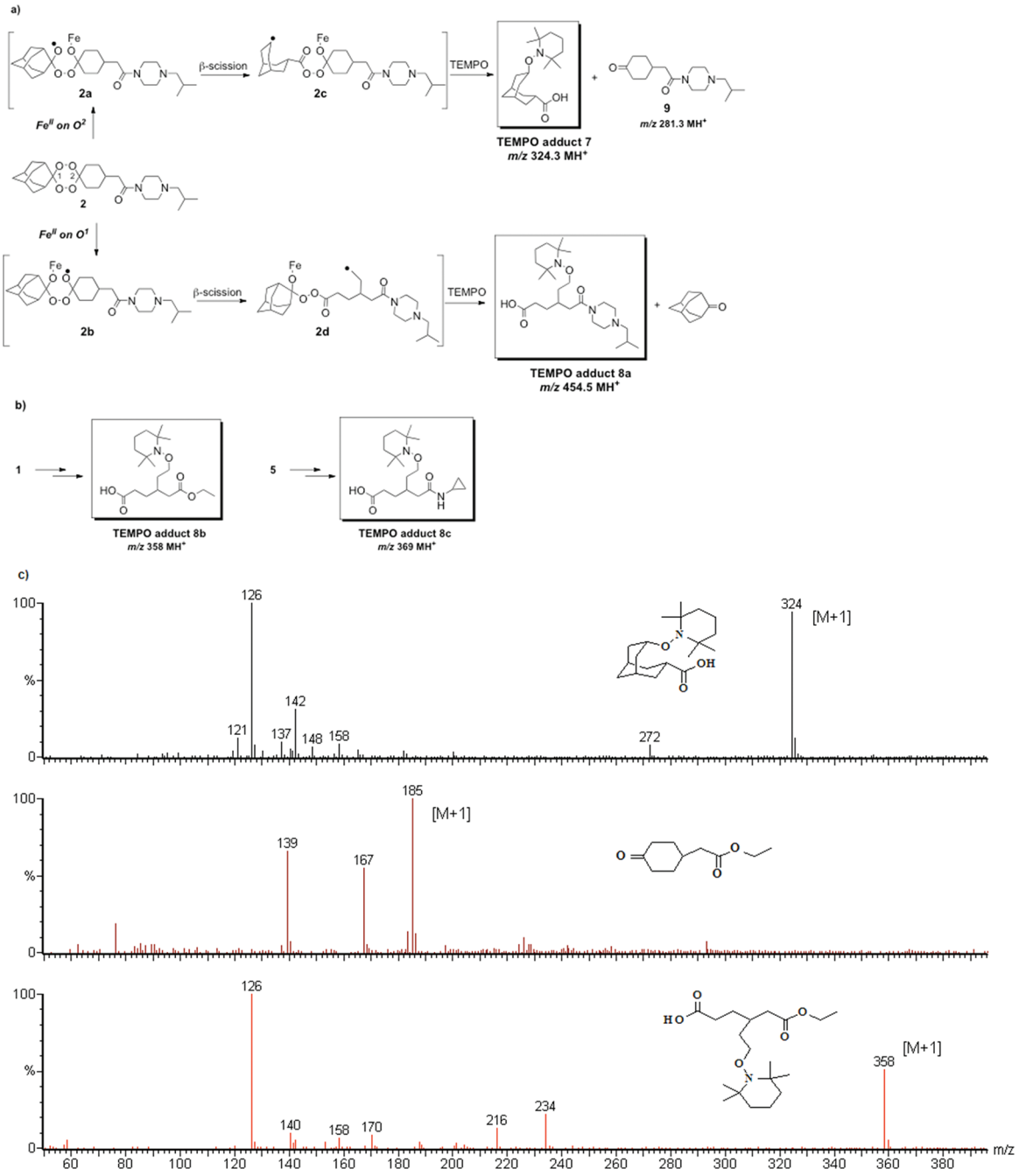


**Figure 3.** (a) Fe-mediated activation of **2** and TEMPO spin-trapping; (b) structures of adducts **8b** and **8c**; and (c) fragmentations of adducts **7** and **8b**.

released during infection, leads to lower than expected drug exposure, and by studying the stability in the presence of infected red blood cells and Fe(II) salts, more stable analogues can be designed and synthesized as exemplified by **16** (OZ439).[22]

## RESULTS AND DISCUSSION

**Reactivity with Fe(II) and TEMPO Spin-Trapping.** In order to confirm the proposition that carbon-centered free radical intermediates are readily produced from our antimalarially active lead 1,2,4,5-tetraoxanes,[19] we set out to perform spin-trapping experiments with 2,2,6,6-tetramethyl-1-piperidine 1-oxyl (TEMPO). Reaction of tetraoxane **2** with ferrous sulfate in the presence of TEMPO in acetonitrile led to the formation of the two TEMPO adducts **7** ($m/z$ 324.3 $MH^+$, Figure 3) and **8a** ($m/z$ 454.5 $MH^+$). The reactivity of the tetraoxanes occurs by coordination of $Fe^{2+}$ with O2 resulting in the formation of the oxyl-radical **2a** (Figure 3). Ring-opening via $\beta$-scission produces the secondary C-radical **2c**, which was trapped with TEMPO to give the adduct **7**, along with the keto-amide **9** ($m/z$ 281.3 $MH^+$). Alternatively, coordination on O1 leads to the formation of the oxy radical **2b** that rearranges to the primary C-radical **2d**, also trapped with TEMPO to give the product **8a**. Similar experiments were carried out with tetraoxanes **1** and **5** in the presence of $FeBr_2$ in THF. From these experiments, the adduct **7** was identified in both cases. Analogous to the adduct **8a**, adducts **8b** and **8c** were also


dx.doi.org/10.1021/jm200768h |J. Med. Chem. 2011, 54, 6443–6455

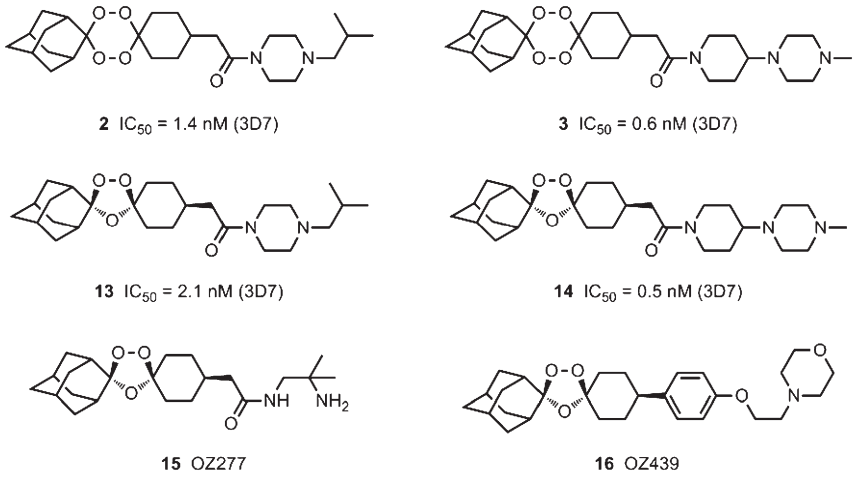


**Figure 4.** Tetraoxanes **2** and **3** and their trioxolane analogues **13** and **14**, respectively, as well as **15** (OZ277) and **16** (OZ439).

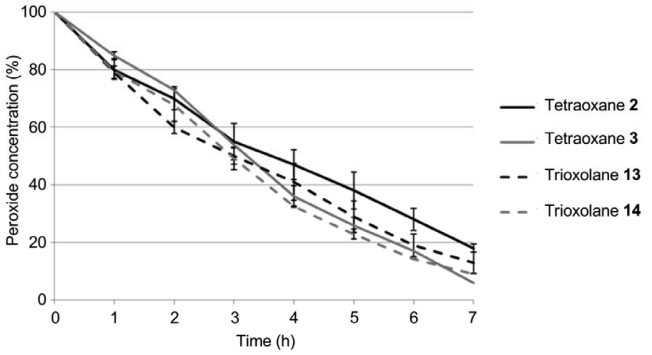


**Figure 5.** Time-dependence profile for the decomposition of peroxides by 18 equiv of $FeSO_4$ in aqueous acetonitrile.

characterized after trapping of the primary radical derived from **1** and **5**, respectively (Figure 3b,c).

The identification of the two TEMPO adducts **7** and **8a** provided evidence for the formation of two carbon-centered radicals after iron(II) activation of tetraoxanes, a similar feature observed with artemisinin. Our experiments provide results that are clearly distinct from previous work on steroidal 1,2,4,5-tetraoxanes where Opsenica et al. reported the generation of oxyl radical species that do not undergo any further rearrangement to form carbon-centered radicals.[23] Second, while experiments with trioxolanes like **15** (Figure 4) resulted in the identification of only secondary radicals,[24] we observed the formation of both primary and secondary carbon centered radicals in the presence of inorganic ferrous salts. Thus, while the overall rates of degradation with excess $FeSO_4$ are similar (Figure 5), tetraoxanes can generate two C-radical species following activation.

While spin-trapping and LC-MS analysis of adducts provides a qualitative view of reactivity, quantitative measurements of each spin-trapped adduct proved difficult due to the high polarity of adducts **8a**−**8c**. To achieve a quantitative assessment, we employed a more lipophilic fluorinated tetraoxane derivative **6** using iron(II) gluconate as the reductant (Figure 6). In this study, performed in the absence of a spin-trap, we obtained **10** and **12** in yields of 44% and 51%, both of which were purified by column chromatography. We propose that H-abstraction from DMF by **6c** facilitates the formation of **10**. While we demonstrate that the C-radical **6d** has the ability to alkylate heme, react with nitroso spin-traps, and potentially abstract hydrogens from lipids, as shown in Figure 8, an intramolecular attack on the peroxy ester function by the C-radical center of **6d** can readily yield the lactone **11a** with loss of $FeO^{3+}$ with the formation of the observed amide **12**. Closer examination of the LCMS data revealed that lactone **11a** was indeed generated under these reaction conditions (Figure S1, Supporting Information). To be absolutely certain that the H-abstraction product **11b** was not produced under these conditions, an authentic synthesis of **11b** was performed to provide a standard for LCMS analysis (Supporting Information). With an authentic sample of **11b**, we were able to rule out the generation of this product under the reaction conditions. Additional studies with $FeSO_4$ in acetonitile-water also revealed that **10**, **12**, and adamantanone are readily produced under aqueous conditions (Figure S2, Supporting Information).

**Ferrous Salt-Mediated Reactivity: Tetraoxane vs Trioxolanes.** For the purposes of direct comparison, we prepared the trioxolanes **13** and **14**, analogues of tetraoxanes **2** and **3**, respectively, in order to compare the stability and the reactivity of the 1,2,4,5-tetraoxane pharmacophore to the ozonide core in the presence of iron(II) using standard conditions (Figure 4).

Iron-mediated decomposition was observed for both tetraoxanes and trioxolanes. The time-dependent degradation studies, conducted by monitoring the loss of parent endoperoxide by LC-MS, showed a linear decrease in tetraoxane concentration (Figure 5). Similar reaction profiles were observed for tetraoxanes and trioxolanes, indicating that the stability of the two classes of drugs with inorganic Fe(II) is comparable. The results observed for these pairs of endoperoxides is in sharp contrast to studies comparing the reactivity of sulfonamide based tetraoxanes where tetraoxanes proved to be considerably more stable than their trioxolane counterparts (note that this previous study used lower equivalents of Fe(II) salts).[18] This observation emphasizes the important role of the side chain in influencing endoperoxide drug stability, and such effects have been seen in the C-10 amino semisynthetic artemisinin derivatives studied by Haynes.[25] Clearly by design, it is possible to tune the reactivity of endoperoxides by the incorporation of appropriate side-chains; a point exemplified by the discovery of **16**, a molecule with enhanced Fe(II) stability preventing plasma-mediated decomposition in infected patients and an outstanding antimalarial activity profile.[22]

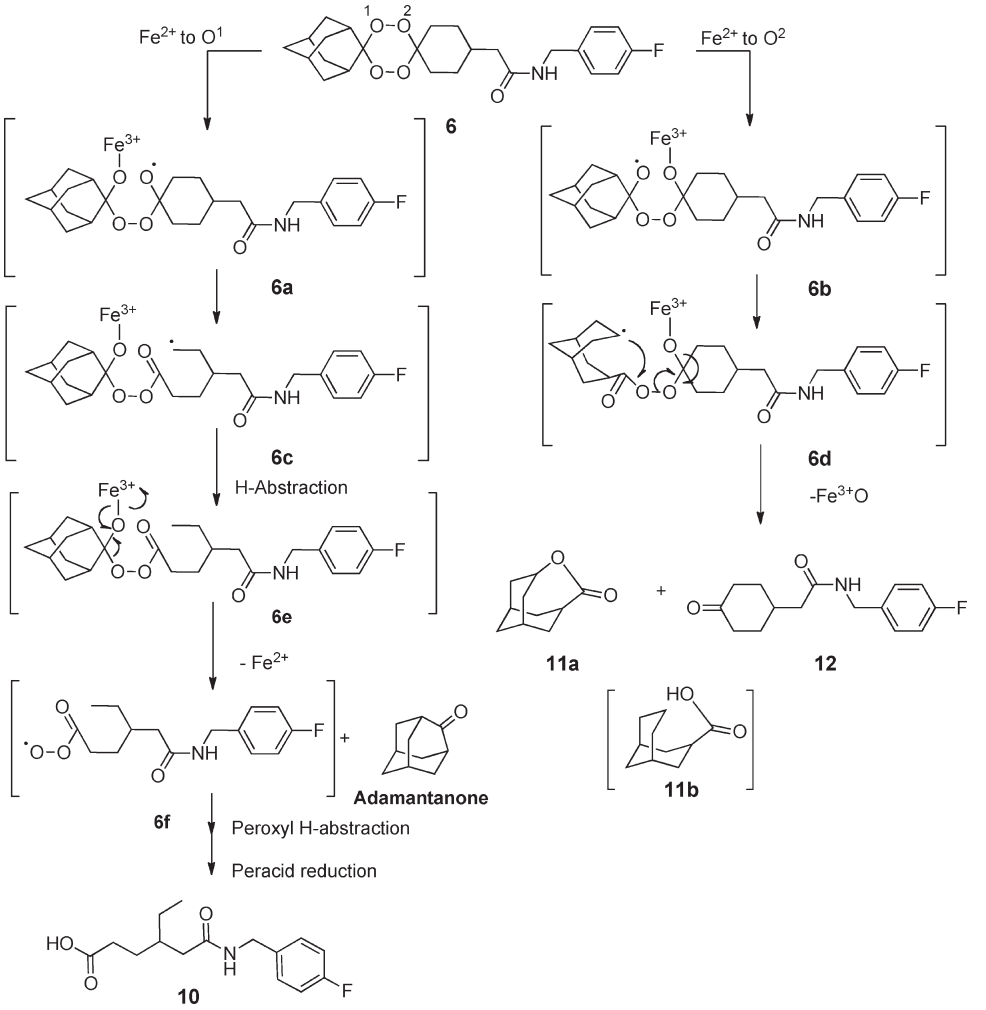


**Figure 6.** Fe(II)-mediated degradation of fluorophenyl amide tetraoxane **6**.

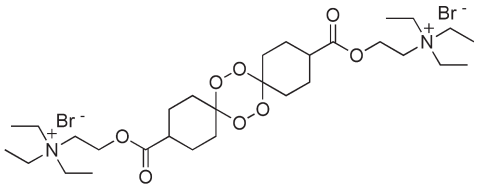


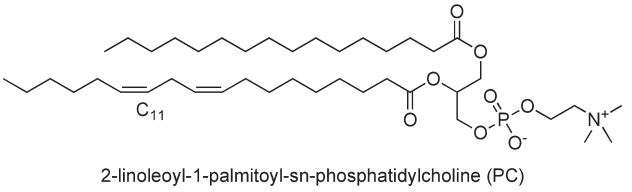


**Figure 7.** Structures of the symmetrical salt previously studied and 2-linoleoyl-1-palmitoyl-*sn*-phosphatidylcholine (PC).

**Reactivity of Tetraoxanes with Fe(II) and Phosphatidylcholine (PC).** Since the proposal that C-centered radicals can alkylate proteins has been met with scepticism, we were keen to investigate the capacity of tetraoxanes and trioxolanes to H-abstract from biologically relevant lipid targets as an alternative potential mechanism of action. Both the primary and secondary C-radicals, produced after tetraoxane activation, may react in vivo with lipids of the membrane bilayer, a well-known target for reactive oxygen species (ROS), leading to cell damage and death. Kumura and colleagues have recently reported that water-soluble structurally distinct tetraoxane salts (Figure 7) can induce olefin oxidative degradation in the presence of an Fe(II) salt. Several PC degradation products were identified, but no mechanisms were proposed for their formation.[20] Since the structure of this salt is very different from our unsymmetrical more lipid soluble 1,2,4,5-tetraoxanes, it was considered vital to examine the reactivity of our lead molecules in this system. The validity of using PC as a target lipid is exemplified by the work of Tilley, who examined the nature of the lipid environment within *Plasmodium falciparum*, which included analysis of the food vacuole and associated food vacuole lipid bodies.[21] These studies reveal the presence of PC in the parasite food vacuole, the site of heme production. We studied the reactivity of tetraoxanes **2** and **3** with PC, under Fenton reaction conditions, and we compared this reactivity with that of trioxolane analogues, **13** and **14**, respectively.

2-Linoleoyl-1-palmitoyl-*sn*-phosphatidylcholine (PC) is composed of a phosphocholine polar head linked to the glycerol moiety with palmitic acid, a saturated fatty acid chain at the *sn*-1


dx.doi.org/10.1021/jm200768h |*J. Med. Chem.* 2011, 54, 6443–6455

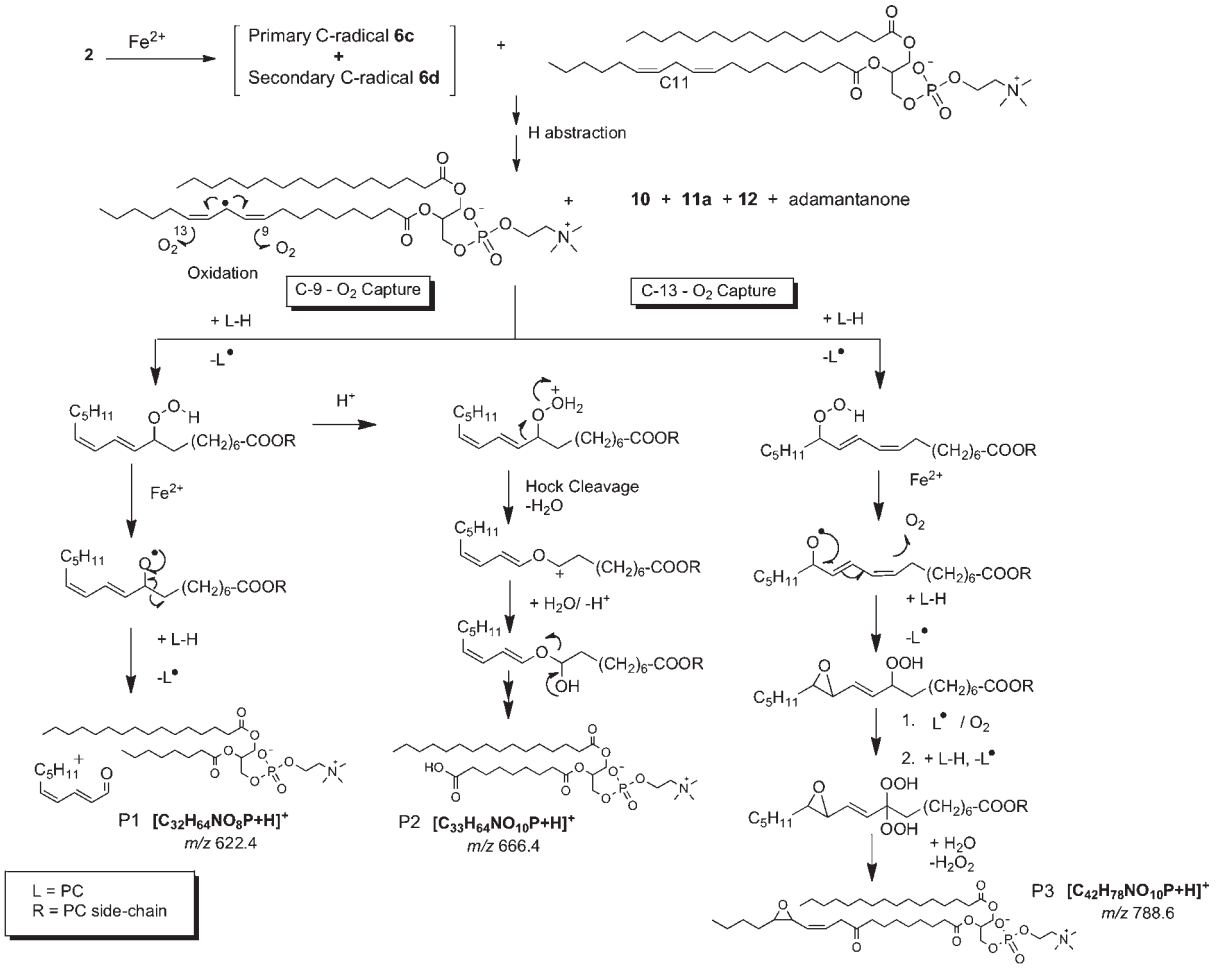


**Figure 8.** Proposed mechanisms for tetraoxane-mediated lipid peroxidation with structures suggested by Kumura et al.[20]

position, and linoleic acid, an unsaturated fatty acid chain at the *sn*-2 position (Figure 7).

Reactions of PC ($m/z$ 758 $M^+$) with tetraoxanes **2** and **3** in the presence of ferrous sulfate led to the formation of several products, different from the native PC. LC-MS analysis showed the predominant degradation products had $m/z$ 622.4, 666.4, 788.6 (810.5), and 808.5. All of these ions, except $m/z$ 808.5, were detected by Kumura.[20] The structures proposed for the PC oxidation products are depicted in Figure 8. The ketone (**9** when tetraoxane **2** was used) was also identified as a byproduct of the reaction. The bis-allylic hydrogen at C11 of the linoleic acid is more likely to be abstracted by the tetraoxane-derived radicals, and we have rationalized the formation of each of these products according to the mechanisms depicted in Figure 8 on the basis of considerations of the extensive mechanistic studies of Spiteller[26] and Domingues.[27,28] Product **P1** is derived from the C-9 capture of the triplet oxygen followed by the peroxyl radical H-abstraction from another molecule of PC. Homolytic cleavage of the hydroperoxide and fragmentation provides a primary PC derived lipid C-radical on C-8, which abstracts a hydrogen to produce the observed product. Product **P2** is derived via Hock cleavage and generation of an aldehyde, which we proposed is oxidized under the reaction conditions to provide **P2**. Product **P3** with $m/z$ 788.6 is produced from PC by C-11 $O_2$ capture, reductive activation by $Fe^{2+}$ to produce a peroxy epoxide that can readily undergo further H-abstraction, and oxidation to produce a gem-dihyroperoxide, which ultimately collapses to provide the observed product **P3** with the expulsion of hydrogen peroxide.

The reaction with PC was carried out with trioxolanes **13** and **14** under the same conditions, and product analysis indicated that the same PC degradation products were produced indicating that in these conditions the two classes of antimalarials exhibit similar reactivity toward phospholipids.

Having performed these initial studies with the tetraoxane amide **2**, we extended our mechanistic work to the fluoro analogue **6** in order to pinpoint which of the carbon radical species might be responsible for lipid peroxidation via hydrogen atom abstraction from the C-11 of PC. This molecule is currently of interest since it has a potent in vitro antimalarial activity of 3.0 nM versus the 3D7 strain and oral activity versus *Plasmodium berghei* (Supporting Information). An experiment was performed using **6** with PC and monitored using ESI/MS to determine the tetraoxane degradation products. ESI/MS revealed the same lipid peroxidation products depicted in Figure 8 along with acid **10**, adamantanone, and lactone **11a**; notably, acid **11b** was not detected. The data obtained from this experiment suggests strongly that the primary radical **6c** is the likely mediator of hydrogen abstraction in these reactions, although we cannot rule out the role of **6d** as the initiator since only catalytic quantities may be required to set in motion the pathway of PC breakdown depicted in Figure 8.

Under the same reaction conditions with artemisinin, native PC was found intact, confirming that artemisinin does not


dx.doi.org/10.1021/jm200768h |*J. Med. Chem.* 2011, 54, 6443–6455

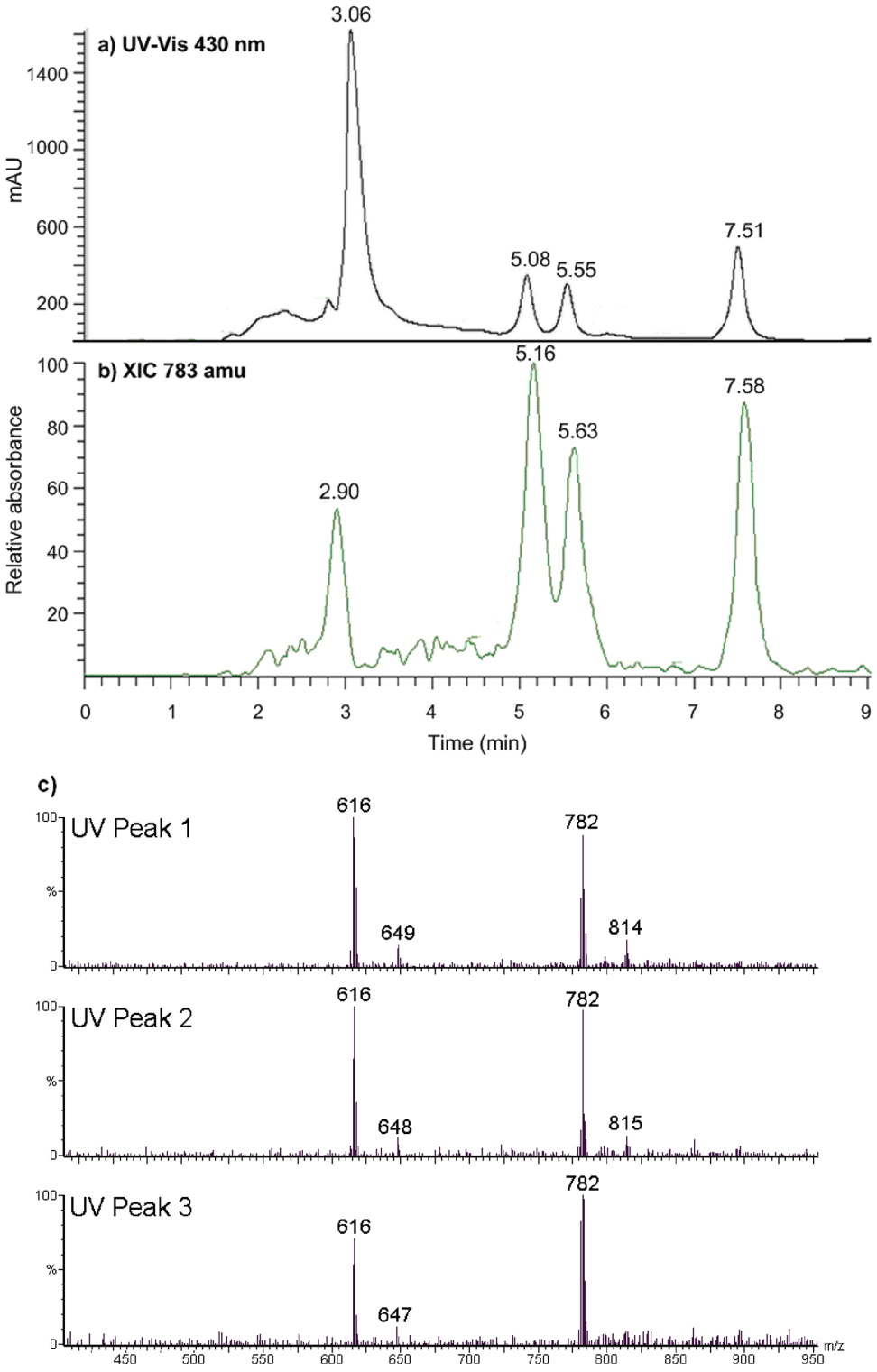


**Figure 9.** (a) UV−vis trace; (b) extracted ion chromatogram at $m/z$ 783.2 of the reaction of heme with tetraoxane; and (c) mass spectra of the heme adducts.

produce phospholipid oxidation in a manner similar to the other endoperoxides examined. With heme as the activator, artemisinin has been shown to enhance the heme-mediated lipid membrane damage[29] but did not affect PC in our nonheme conditions. This difference of reactivity between artemisinin and tetraoxanes/trioxolanes here may be due to the difference in the stability of the radical intermediates. The artemisinin-derived radicals are more reactive, and the intramolecular rearrangement of these radicals may be too rapid for intermolecular H-bond abstraction from lipids.

**Reactivity of Tetraoxanes with Heme.** Several studies have shown that iron(II)-heme quickly reacts with the peroxide bond


dx.doi.org/10.1021/jm200768h |*J. Med. Chem.* 2011, 54, 6443–6455

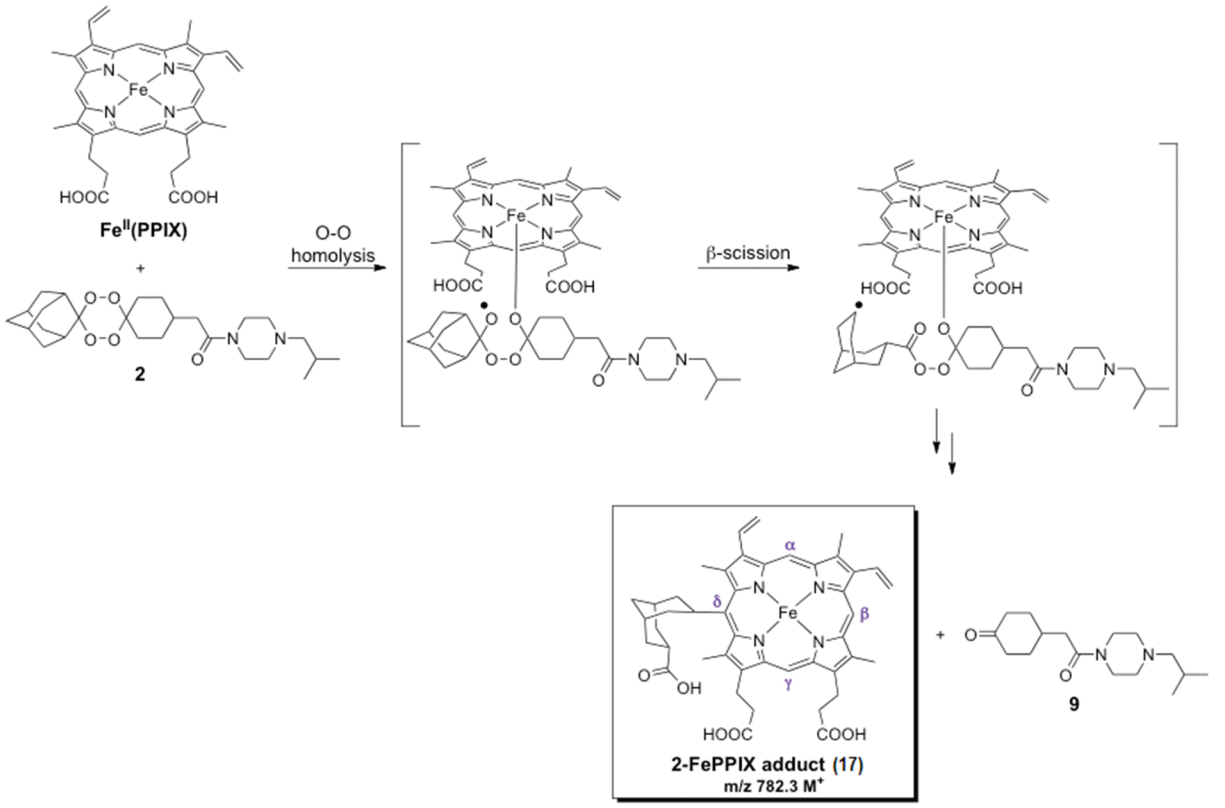


**Figure 10.** Proposed mechanism for the alkylation of heme (Fe(II)-PPIX) by tetraoxane **2**. Adapted with permission from ref 31. Copyright 2008 American Society for Microbiology.

of various synthetic endoperoxide antimalarials. The pathways are mechanistically similar to those described with ferrous ions with the exception that the generated C-centered radicals tend to react in an intramolecular fashion with the porphyrin macrocycle to form heme-drug adducts. Such adducts have been isolated and/or characterized with artemisinin[8] and other antimalarial peroxides.[30−32]

We investigated the reaction of tetraoxanes **2** and **3** with ferrous-heme and found that the peroxides rapidly react with the porphyrin. In both cases, HPLC analysis of the crude mixture showed that most of the starting heme had reacted within 30 min, giving three products with higher retention times than the heme itself (Figure 9a) and a maximum absorption of the Soret band at 430 nm, instead of 398 nm for heme. LC-MS analysis showed that these three compounds exhibit a $m/z$ 782.3 ($M^+$), consistent with covalent coupling products (**17**, Figure 10) formed between heme (mass 616) and the tetraoxane-derived secondary C-centered radical **2c**. The same alkylated heme adduct has been reported with trioxolanes in similar conditions by Creek et al.[31] The extracted ion chromatogram at $m/z$ 782.3 showed four peaks (Figure 9b) expected to be the four possible regio-isomers of the alkylated heme adduct **17**, as reported by Robert et al. for heme-artemisinin adducts.[33]

Similar results were obtained with all the active antimalarial tetraoxanes tested, including **3** and **4** (results not shown). The ketoamide compound, a coproduct of the reaction, was also detected in all cases. We monitored the conversion of heme during the reaction (Figure 11). As a control, the reaction was carried out without the drug, to estimate the loss of heme due to the degradation by residual oxygen. Reaction with artemisinin

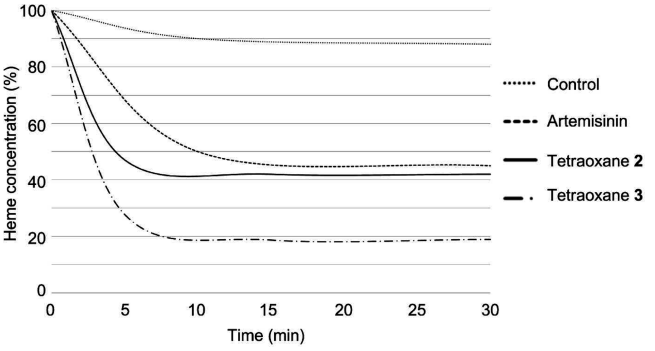


**Figure 11.** Time-dependence profile for the conversion of heme with peroxides.

showed that c.a. 70% of the starting heme was converted within 15 min. Reaction with tetraoxanes **2** and **3** was also rapid and resulted in the conversion of the starting heme of 53% and 38%, respectively, after only 5 min. Concentration−time profiles of heme showed that the reaction is complete within 15 min, as the absorbance of the Soret band remains constant beyond this time point.

Reaction of the direct trioxolane analogues with heme in the same conditions showed a very similar profile, and the same coupling products were identified (Figure 12). However, the adduct formation appeared to be more rapid with trioxolane **13**, and the peak ratio was different. The reaction with heme occurs much faster than the reaction with ferrous sulfate; indeed, tetraoxanes were degraded in a few minutes, while reaction with

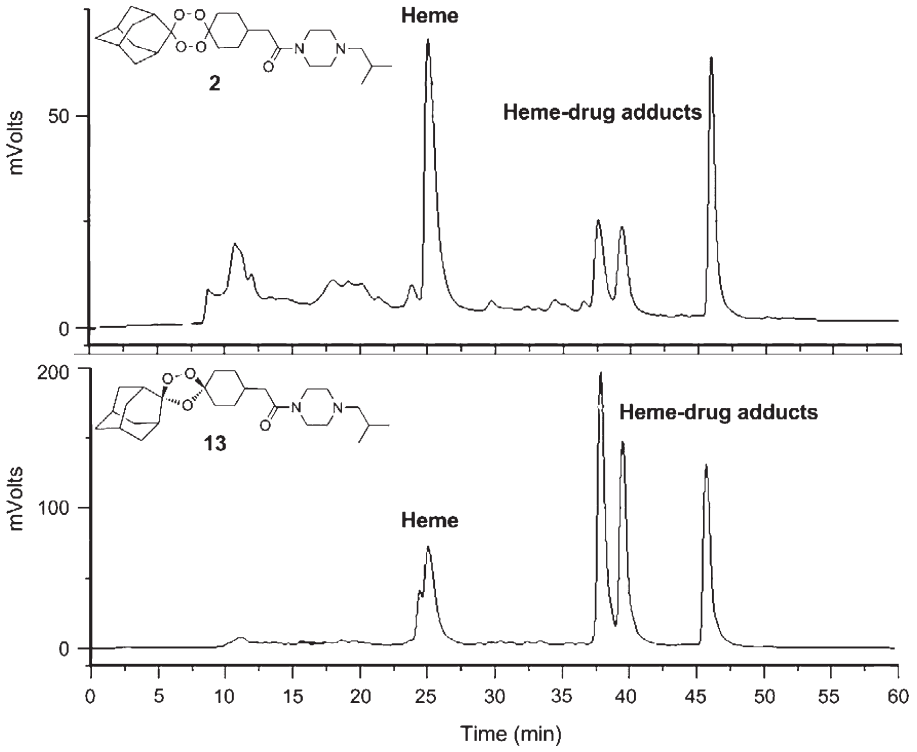


**Figure 12.** LC trace of the reaction mixture of tetraoxane **2** (top) and trioxolane **13** (bottom) with heme.

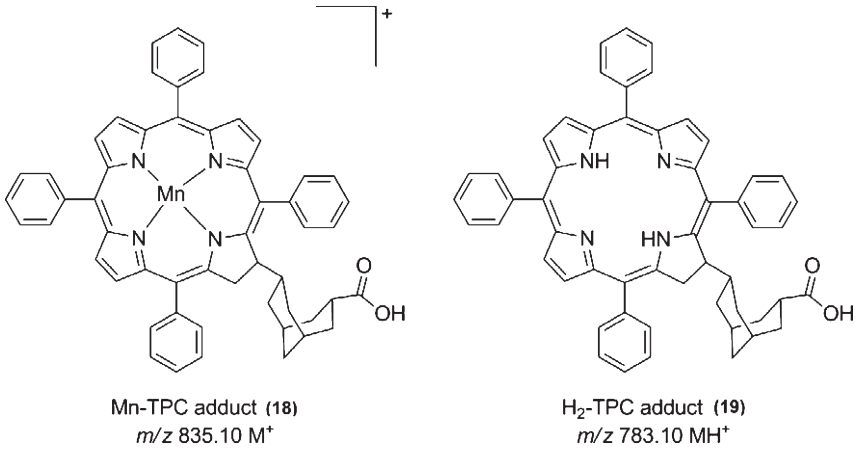


**Figure 13.** Expected structures of Mn-TPC- and $H_2$-TPC-tetraoxane adducts **18** and **19**.

inorganic iron requires several hours. This increased reaction rate is also observed with trioxanes and trioxolanes.[31,32]

Because of their low stability, quantification of the adducts was not possible. However, the estimated yield of adducts after 15 min for **2** is 34%, which is about half of the yield observed with **13** in the same conditions (71%).[34] No significant differences were observed between **3** and **14** (data not shown).

As reported with artemisinin, we also studied the alkylating activity of tetraoxanes with iron(II) tetraphenylporphyrin and manganese(II) tetraphenylporphyrin, two symmetrical synthetic porphyrins, to confirm the results observed with heme.[35] Reaction of tetraoxane **2** with $Mn^{II}$TPP gave a porphyrin-drug adduct with $m/z$ 835.10 ($M^+$), consistent with a chlorin-type adduct (**18**). This adduct results from alkylation on one of the eight $\beta$-pyrrolic positions of the macrocycle by the tetraoxane-derived secondary radical. The same chlorin-type adduct was identified after reaction with $Fe^{II}$TPP. The demetalated adduct **19** (Figure 13) was also identified ($m/z$ 783.10, $MH^+$) after workup and Mn removal. These results with the tetraphenylporphyrins confirm the alkylating capacity of antimalarial tetraoxanes observed with heme.

One can note that, although the primary and the secondary radical can possibly be generated after reduction by $Fe^{2+}$ salts, only the tetraoxane-derived secondary radical (**2c**) was found to react with heme and tetraphenylporphyrins. In the case of artemisinin and other trioxanes, only adducts resulting from the primary radical were reported.[8,32] This could be explained by the relative positions of the peroxide bond and the porphyrin ligand. Contrary to free iron, which can coordinate both oxygen atoms, iron in the heme porphyrin would less easily coordinate O1,


dx.doi.org/10.1021/jm200768h |J. Med. Chem. 2011, 54, 6443–6455

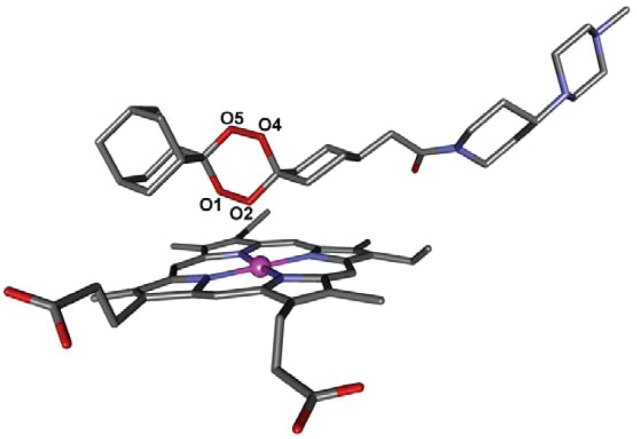


**Figure 14.** Docking configuration between heme and RKA182 (**3**).

which is close to the bulky adamantane group. However, we cannot rule out the possibility that the primary radical is also formed but does not react with the porphyrin.

To confirm the hypothesis that the two oxygens (O2 and O4) preferentially coordinate to the heme iron center, we performed a modeling study of the interaction between heme and tetraoxane **3**. The objective here was to see whether the regioselectivity of the alkylation reaction could be predicted by docking calculations. For this purpose, we used the AutoDock 4.0 software[36] with two different protocols: in the first procedure, the heme receptor was kept fully rigid, while in the second protocol, the two propionate chains of the protoporphyrin were left flexible. In both cases, docked conformations showed that heme preferentially interacts with the tetraoxane via the O2 atom, rather than the alternative O1 atom. For **3**, conformation depicted in Figure 14, the O1−O2 bond and the amide side chain are at equatorial positions of the cyclohexyl ring, e.g., trans to each other, making this peroxide accessible to the $Fe^{2+}$ center of the porphyrin (Figure 14). In all docking conformations, the shortest distance between iron heme and **3** was found to be with O2, ranging from 2.4 Å to 2.8 Å for the lowest energy conformations (27/50) suggesting a preferred coordination of Fe on the sterically less-hindered oxygen atom O2 of the peroxide bond of **3**, confirming the regioselectivity observed in alkylation experiments.

## CONCLUSIONS

Iron(II)-mediated activation of tetraoxanes results in the formation of a primary and a secondary C-centered radical, in contrast to 1,2,4-trioxolanes and the stability of 1,2,4,5-tetraoxanes studied here, in the presence of nonheme ferrous iron, is dependent on the nature of the amide side chain. Overall the stability of tetraoxanes is comparable with that of their trioxolane counterparts (when substituted with identical side chains), and both classes of drugs react with PC to give peroxidation products after reductive activation by $Fe^{2+}$. On the basis of products identified from the activation chemistry in these reactions, it appears that for tetraoxanes the pathway of lipid peroxidation involves lipid H-abstraction by C-radical intermediates. All of the tetraoxanes used in this study were shown to rapidly react with Fe(II)-heme; the major reaction products are alkylated heme adducts, resulting from the addition of the adamantane-derived secondary C-radical intermediate. Docking studies with heme provide a plausible explanation for the regioselectivity observed in the association of the endoperoxide bridge with a preference for the association of the least hindered atom O2 with heme $Fe^{2+}$. The high reactivity with heme and the formation of covalent heme-drug adducts are features shared by all tested active semisynthetic artemisinins and trioxolane and tetraoxane derivatives; the role of this event in the antimalarial mechanism remains to be clarified. The establishment that the front line synthetic artemisinin replacements efficiently promote lipid peroxidation has potential implications for both mechanism of action and potential drug safety, and studies in *Plasmodium falciparum* and susceptible human cell lines (e.g., neuronal cells, embryonic cell lines) are warranted in the near future.

## EXPERIMENTAL SECTION

**LC-MS Analysis.** Mass spectrometry analysis was performed on a Thermo TSQ Quantum Access triple quadrupole mass spectrometer connected to a LC device Thermo Accela high pressure pump, auto sampler, and PDA detector. Analytical separations were performed on a 150 × 3 mm Thermo Hypersyl HyPURITY C18 column (5 $\mu$m). Data were captured in full MS scan mode and processed using Xcalibur software (version 2.0.7) and a Thermo Quan browser (version 2.0.7).

**Chemistry.** All reagents were purchased from Sigma Aldrich UK and were used without purification. NMR spectra were recorded on a Bruker AMX 400 ($^1$H, 400 MHz; $^{13}$C, 100 MHz) spectrometer, using $CDCl_3$ or $d_4$-MeOD as the solvent. Chemical shifts are described in ppm ($\delta$) downfield from an internal standard of trimethylsilane. Tetraoxanes 1, 4, 5, and 6 were prepared according to the procedure reported by Amewu et al.[17] The purity of all target compounds was >95% as confirmed by combustion analysis.

**Synthesis of Tetraoxanes 2 and 3.** Tetraoxanes **2** and **3** were prepared according to the method reported by O'Neill et al.[19]

**Synthesis of Tetraoxane 6.** Tetraoxane **6** was prepared according to the procedure reported by Amewu et al.[17] using 4-fluorobenzylamine in the coupling step. White solid (0.190 g, 426 $\mu$mol, 71%); $^1$H NMR (400 MHz, $CDCl_3$) $\delta$ 7.29−7.20 (m, 2H), 7.01−6.98 (m, 2H), 5.70 (s, 1H), 4.41 (d, $J$ = 5.7 Hz, 2H), 2.11 (d, $J$ = 7.1 Hz, 2H), 2.07 − 1.91 (m, 5H), 1.90−1.83 (m, 3H), 1.82−1.66 (m, 7H), 1.66−1.50 (m, 4H), and 1.45−1.15 (m, 2H). $^{13}$C NMR (101 MHz, $CDCl_3$) $\delta$ 171.8, 162.3 (d, $J$ = 245.0 Hz), 129.6 (d, $J$ = 8.1 Hz), 115.7 (d, $J$ = 21.5 Hz), 110.6, 107.8, 43.5, 43.0, 37.1, 34.2, 33.3, and 27.2. Mp = 146 °C; IR 3242, 3072, 2918, 2856, 2370, 2341, 1631, 1545, 1510, 1448, 1375, 1302, 1225, 1176, 1101, 1061, 999, 928, 829, 741, 685, and 613 cm$^{-1}$. HRMS calculated for $C_{25}H_{32}FNO_5$ $[M + Na]^+$, 468.2162; found, 468.2149. Microanalysis calculated for $C_{25}H_{32}FNO_5$: C, 67.40%; H, 7.24%; N, 3.14%. Found: C, 67.66%; H, 7.28%; N, 3.15%.

**Synthesis of Trioxolanes 13 and 14.** *cis*-Adamantane-2-spiro-3′-8′-(carboxymethyl)-1′,2′,4′-trioxaspiro[4.5]decane was prepared according to the method reported by Vennerstrom.[37]

Preparation of *cis*-adamantane-2-spiro-3′-8′-[1-(2-methylpropyl)piperazino]-1′,2′,4′-trioxaspiro[4.5]decane (**13**): To a solution of *cis*-adamantane-2-spiro-3′-8′-(carboxymethyl)-1′,2′,4′-trioxaspiro[4.5]decane (0.5 g, 1.55 mmol) in dry $CH_2Cl_2$ (50 mL) at 0 °C were added $Et_3N$ (0.44 mL, 3.10 mmol, 2 equiv) and methyl chloroformate (0.12 mL, 1.55 mmol, 1 equiv) under $N_2$. The mixture was stirred at 0 °C for 1 h, and 1-(2-methylpropyl)piperazine was added (0.22 mL, 1.55 mmol, 1.0 equiv). The reaction mixture was stirred at 0 °C for 45 min and at rt for another 2 h. The reaction mixture was diluted with 50 mL of water and extracted with $CH_2Cl_2$ (2 × 60 mL). The organic layers were combined and washed with water (40 mL) and brine (40 mL), dried on $Na_2SO_4$, and evaporated in vaccuo. The crude product was purified by flash chromatography (silica gel, eluent, ethyl acetate/$CH_2Cl_2$ 50:50) to afford trioxolane **13** (0.48 g, 70%) as a white solid.

$^1$H NMR (500 MHz) $\delta$ 3.64 (bs, 2H), 3.48 (bs, 2H), 2.39 (bs, 4H), 2.23 (d, $J$ = 6.9 Hz, 2H), 2.10−1.60 (m, 24H), 1.26 (dq, $J$ = 13.2 and 5.4 Hz, 2H), 0.93 (d, $J$ = 6.6 Hz, 6H); $^{13}$C NMR (125 MHz) $\delta$ 170.4, 111.1, 108.6, 66.7, 53.9, 53.3, 45.8, 41.6, 39.1, 36.9, 36.5, 34.8, 34.1, 33.4, 30.3, 26.9, 26.6, 25.4, 20.8. HRMS calculated for $C_{26}H_{43}N_2O_4$ $[M + H]^+$: 447.3223. Found: 447.3221. Elemental analysis, C: 70.16, H: 9.61, N: 6.40 (required values, C: 69.92, H: 9.84, N: 6.40).

Preparation of *cis*-adamantane-2-spiro-3′-8′-[1-methyl-4-(4-piperidino)-piperazino]-1′,2′,4′-trioxaspiro[4.5]decane (**14**): To a solution of *cis*-adamantane-2-spiro-3′-8′-(carboxymethyl)-1′,2′,4′-trioxaspiro[4.5]decane (1.5 g, 4.65 mmol) in dry $CH_2Cl_2$ (150 mL) at 0 °C were added $Et_3N$ (1.32 mL, 9.30 mmol, 2 equiv) and methyl chloroformate (0.36 mL, 4.65 mmol, 1 equiv) under $N_2$. The mixture was stirred at 0 °C for 1 h, and 1-methyl-4-(4-piperidino)piperazine was added (860 mg, 4.69 mmol, 1 equiv). The reaction mixture was stirred at 0 °C for 30 min and at rt for other 2 h. The reaction mixture was diluted with 150 mL of water and extracted with $CH_2Cl_2$ (3 × 100 mL). The organic layers were combined and washed with water (100 mL) and brine (100 mL), dried on $Na_2SO_4$, and evaporated in vaccuo. The crude product was purified by flash chromatography (silica gel, eluent, $CHCl_3$/methanol 100:0 to 90:10) to afford trioxolane **14** (418 mg, 20%) as a white solid.

$^1$H NMR (500 MHz) $\delta$ 4.65 (bd, $J$ = 12.8 Hz, 2H, $CH_2$), 3.92 (bd, $J$ = 13.3 Hz, 2H, $CH_2$), 3.01 (t, $J$ = 12.8 Hz, 2H), 2.70−2.39 (m, 7H, CH/$CH_2$), 2.31 (s, 3H, $NCH_3$), 2.23 (d, $J$ = 6.9 Hz, 2H), 2.03−1.25 (m, 27H, CH/$CH_2$); $^{13}$C NMR (125 MHz) $\delta$ 170.2, 111.3, 108.7, 61.7, 55.4, 49.0, 45.9, 45.1, 41.1, 39.2, 36.9, 36.5, 34.8, 34.1, 33.4, 30.3, 29.2, 28.3, 26.9, 26.6. HRMS calculated for $C_{28}H_{46}N_3O_4$ $[M + H]^+$, 488.3488. Found: 488.3487. Elemental analysis, C: 68.76, H: 9.00, N: 8.60 (required values, C: 68.96, H: 9.30, N: 8.62).

**General Procedure for the Reaction of Tetraoxanes with $Fe^{2+}$ and TEMPO.** A solution of tetraoxane (0.5 mmol), $FeSO_4$ or $FeBr_2$ (2 equiv), and TEMPO (2 equiv) in THF or $CH_2Cl_2/CH_3CN$ 50:50 (10 mL) was stirred at ambient temperature under nitrogen atmosphere for 24 h and concentrated. The crude product was dissolved in ethyl acetate, washed with water and brine, dried over $MgSO_4$, filtered, and concentrated. The crude product was analyzed by LC-MS, and TEMPO adducts were identified in all cases.

**General Procedure for the Reaction of Antimalarial Peroxides with Ferrous Sulfate.** Stock solution of peroxide (10 mM in absolute ethanol) and ferrous sulfate (100 mM in water) were freshly prepared and degassed prior to use. A solution of ferrous sulfate (1.0 mL, 18.2 mM) was added to a solution of peroxide (1.0 mL, 1 mM) in ACN/$H_2O$ 1:1 (final volume 5.5 mL). The reactions were allowed to stir at room temperature under nitrogen with LC-MS monitoring.

LC-MS analysis: Compounds were eluted using a ternary solvent system consisting of 50% MeOH, 35% acetonitrile, and 15% 0.1 M ammonium acetate in isocratic mode (flow rate: 0.5 mL/min).

**General Procedure for the Reaction of Tetraoxane 6 with Iron(II) Gluconate.** To a stirred solution of **6** (0.200 g, 449 $\mu$mol) in water (5 mL) and dimethylformamide (20 mL) under nitrogen atmosphere, Fe(gluconate)$_2$ (0.400 g, 898 $\mu$mol, 2 equiv) was added. The mixture was left to stir for 12 h at room temperature. Dimethylformamide was removed in vacuo and the crude product extracted with dichloromethane (3 × 20 mL). The combined organic extracts were washed with brine, dried over magnesium sulfate, and concentrated in vacuo to give the crude product. Purification by flash column chromatography (silica gel, 1:1 ethyl acetate/dichloromethane) obtained **10** (56.4 mg, 44.6%) and **12** (61.2 mg, 51.7%) as white solids.

Data for **10**: $^1$H NMR (400 MHz, $d_4$-MeOH) $\delta$ 7.45−7.08 (m, 2H), 7.08−6.91 (m, 2H), 6.34 (s, NH), 4.35 (pseudo s, 2H), 2.28 (s, 2H,), 2.20 (s, 2H), 1.85 (s, 1H), 1.58 (s, 2H), 1.29 (s, 2H), and 0.84 (s, 3H); $^{13}$C NMR (100 MHz, $d_4$-MeOH) $\delta$ 178.3, 175.4, 163.4 (d, $J$ = 244 Hz), 136.3 (d, $J$ = 3 Hz), 130.5 (d, $J$ = 8 Hz), 116.1 (d, $J$ = 22 Hz), 43.4, 41.3, 37.8, 32.8, 29.7, 27.0, 11.0; MS (ES+) HRMS calculated for $C_{15}H_{20}FNO_3$ $[M + Na]^+$, 304.1325. Found, 304.1319.

Data for **12**: $^1$H NMR (400 MHz, $CDCl_3$) $\delta$ 7.28−7.22 (m, 2H), 7.08−6.97 (m, 2H), 5.77 (s, NH), 4.43 (d, $J$ = 5.7 Hz, 2H), 2.48−2.32 (m, 6H), 2.24−2.17 (m, 3H), and 2.17−2.05 (m, 2H). $^{13}$C NMR (100 MHz, $CDCl_3$) $\delta$ 211.6, 171.5, 162.3 (d, $J$ = 246.1 Hz), 134.1 (d, $J$ = 3.2 Hz), 129.6 (d, $J$ = 8.0 Hz), 115.7 (d, $J$ = 21.5 Hz), 43.1, 42.8, 40.8, 33.6, 32.7; MS (ES+), HRMS calculated for $C_{15}H_{18}FNO_2$ $[M + Na]^+$, 286.1214. Found 286.1216.

The degradation reaction of tetraoxane **6** (0.100 g, 224 $\mu$mol) was also performed using ferrous sulfate. We obtained **6**, **10**, **12**, and unknown products in yields of 8.9%, 47%, 27%, and 22 mg, which were purified by column chromatography

**Reaction of Antimalarial Peroxides with $FeSO_4$ and PC.** Stock solutions of PC, $FeSO_4$, and peroxides were degassed prior to use. To a solution of PC in water (500 $\mu$L, 0.83 $\mu$mol) were added an aqueous solution of ferrous sulfate (500 $\mu$L, 7.2 $\mu$mol, 8.7 equiv) and a solution of peroxide in absolute ethanol (500 $\mu$L, 6.81 $\mu$mol, 8.2 equiv). For the control reaction, the peroxide solution was replaced by absolute ethanol (500 $\mu$L). The cloudy mixtures were stirred at 38 °C for 24 h under nitrogen atmosphere. An aliquot of each crude mixture was taken for ESI/MS analysis before reactions were quenched with 50% phytic acid solution (10 $\mu$L) and a trace of BHT, according to the procedure reported by Kumura et al.[20] The reaction mixtures were extracted with $CHCl_3/CH_3OH$ (1:2, 1 mL), and the chloroform layers were analyzed by ESI/MS.

**General Procedure for the Reaction of Antimalarial Peroxides with Heme.** Hemin stock solution (10 mM in 0.1 M NaOH) was freshly prepared and degassed with acetonitrile prior to use. Hemin solution (2.0 mL, 0.02 mmol) was added to a solution of peroxide (0.02 mmol, 1 equiv) and dithionite (41 mg, 0.20 mmol, 10 equiv) in acetonitrile (2.0 mL) under argon. The mixture was stirred at room temperature and monitored by LC-MS.

LC-MS analysis: Compounds were eluted using a binary gradient solvent system consisting of MeOH/1% TFA (solvent A) and $H_2O$/1% TFA (solvent B). The gradient used was 70% to 80% of solvent A over 10 min (flow rate: 0.5 mL/min). Retention times were 3.24 min for heme and 5.39 to 8.15 min for the heme-tetraoxane adducts.

**Molecular Docking.** Docking calculations: The docking calculations were carried out using the automated docking program AutoDock 4.0.[36] The grid maps for each atom type found in the ligand structure were calculated using the auxiliary program AutoGrid 4.0. The grid size was set to 100 × 100 × 100 points with 0.375 Å spacing. The Lamarckian genetic algorithm (LGA) was selected for ligand conformational searching. Default parameters were used, except for the number of docking runs, which was set to 50 and the number of evaluations to 10,000,000. Flexible torsion angles in the ligands were assigned with Autotors, an auxiliary module of AutoDock Tools. The resulting docked conformations were clustered into groups of similar binding modes, with a root-mean-square deviation (rmsd) clustering tolerance of 2.0 Å.

Heme and tetraoxane structures: The heme molecule was prepared from hemoglobin crystallographic structure obtained from the Protein Data Bank (pdb code: 2DN1). The Fe oxidation state was 2. RKA182 (**3**) was built using its X-ray structure. The conformation of the 6-membered rings was kept to that of the X-ray structure, e.g., chair conformation. The atomic charges were calculated with the Gaussian suite.[38] The UHF/6-31 g** and HF/6-31 g** basis sets were used for heme and tetraoxane, respectively.

## ■ ASSOCIATED CONTENT

**Supporting Information.** Additional information including the synthesis of **11b**, LCMS methods and traces, determination of antimalarial activity, and the in vivo activity data for **6**.

This material is available free of charge via the Internet at http://pubs.acs.org.

## AUTHOR INFORMATION

**Corresponding Author**

*(P.M.O.) Phone: 00-44-151-794-3553. Fax: 00-44-151-794-3588. E-mail: p.m.oneill01@liv.ac.uk. (F.B.-E.G.) Phone: 00-33-561-333-248. Fax: 00-33-561-553-003. E-mail: bousejra@lcc-toulouse.fr.

## ACKNOWLEDGMENT

We thank Jill Davies (LSTM) for $IC_{50}$ values and Allan Mills (University of Liverpool) for MS analysis. F.B.-E.G. thanks Dr. Anne Robert for helpful discussions and comments and CALMIP (Calcul Intensif en Midi-Pyrénées, Toulouse) for computing facilities. This work was supported by a grant from the EU (Antimal PhD fellowship (to F.B.-E.G.) and FP6Malaria Drugs Initiative (LSHPCT20050188)) and by the Medical Research Council [grant number G0700654] (to M.H.-L.W.).

## ABBREVIATIONS USED

PC, phosphatidylcholine; TPP, tetraphenylporphyrin; ROS, reactive oxygen species; WHO, World Health Organization

## REFERENCES

(1) *World Malaria Report 2009*; World Health Organization: Geneva, Switzerland, 2009.

(2) Greenwood, B. M.; Fidock, D. A.; Kyle, D. E.; Kappe, S. H. I.; Alonso, P. L.; Collins, F. H.; Duffy, P. E. Malaria: Progress, Perils, and Prospects for Eradication. *J. Clin. Invest.* **2008**, *118*, 1266–1276.

(3) Klayman, D. L. Qinghaosu (Artemisinin): An Antimalarial Drug from China. *Science* **1985**, *228*, 1049–1055.

(4) Posner, G. H.; Oh, C. H. A Regiospecifically O-18 Labeled 1,2,4-Trioxane: A Simple Chemical-Model System to Probe the Mechanism-(s) for the Antimalarial Activity of Artemisinin (Qinghaosu). *J. Am. Chem. Soc.* **1992**, *114*, 8328–8329.

(5) Posner, G. H.; Oh, C. H.; Wang, D. S.; Gerena, L.; Milhous, W. K.; Meshnick, S. R.; Asawamahasadka, W. Mechanism-Based Design, Synthesis and In-Vitro Antimalarial Testing of New 4-Methylated Trioxanes Structurally Related to Artemisinin: The Importance of a Carbon-Centered Radical for Antimalarial Activity. *J. Med. Chem.* **1994**, *37*, 1256–1258.

(6) Posner, G. H.; Wang, D. S.; Cumming, J. N.; Oh, C. H.; French, A. N.; Bodley, A. L.; Shapiro, T. A. Further Evidence Supporting the Importance of and the Restrictions on a Carbon-Centered Radical for High Antimalarial Activity of 1,2,4-Trioxanes Like Artemisinin. *J. Med. Chem.* **1995**, *38*, 2273–2275.

(7) Hong, Y. L.; Yang, Y. Z.; Meshnick, S. R. The Interaction of Artemisinin with Malarial Hemozoin. *Mol. Biochem. Parasitol.* **1994**, *63*, 121–128.

(8) Robert, A.; Cazelles, J.; Meunier, B. Characterization of the Alkylation Product of Heme by the Antimalarial Drug Artemisinin. *Angew. Chem., Int. Ed.* **2001**, *40*, 1954–1957.

(9) Meshnick, S. R.; Thomas, A.; Ranz, A.; Xu, C. M.; Pan, H. Z. Artemisinin (Qinghaosu): The Role of Intracellular Hemin in Its Mechanism of Antimalarial Action. *Mol. Biochem. Parasitol.* **1991**, *49*, 181–190.

(10) Asawamahasakda, W.; Ittarat, I.; Pu, Y. M.; Ziffer, H.; Meshnick, S. R. Reaction of Antimalarial Endoperoxides with Specific Parasite Proteins. *Antimicrob. Agents Chemother.* **1994**, *38*, 1854–1858.

(11) Eckstein-Ludwig, U.; Webb, R. J.; van Goethem, I. D. A.; East, J. M.; Lee, A. G.; Kimura, M.; O'Neill, P. M.; Bray, P. G.; Ward, S. A.; Krishna, S. Artemisinins Target the SERCA of *Plasmodium falciparum*. *Nature* **2003**, *424*, 957–961.

(12) Cardi, D.; Pozza, A.; Arnou, B.; Marchal, E.; Clausen, J. D.; Andersen, J. P.; Krishna, S.; Moller, J. V.; le Maire, M.; Jaxel, C. Purified E255L Mutant SERCA1a and Purified PfATP6 Are Sensitive to SERCA-type Inhibitors but Insensitive to Artemisinins. *J. Biol. Chem.* **2010**, *285*, 26406–26416.

(13) Bousejra-El Garah, F.; Stigliani, J. L.; Cosledan, F.; Meunier, B.; Robert, A. Docking Studies of Structurally Diverse Antimalarial Drugs Targeting PfATP6: No Correlation between in Silico Binding Affinity and in Vitro Antimalarial Activity. *ChemMedChem* **2009**, *4*, 1469–1479.

(14) Haynes, R. K.; Chan, W. C.; Wong, H. N.; Li, K. Y.; Wu, W. K.; Fan, K. M.; Sung, H. H. Y.; Williams, I. D.; Prosperi, D.; Melato, S.; Coghi, P.; Monti, D. Facile Oxidation of Leucomethylene Blue and Dihydroflavins by Artemisinins: Relationship with Flavoenzyme Function and Antimalarial Mechanism of Action. *ChemMedChem* **2010**, *5*, 1282–1299.

(15) Haynes, R. K.; Cheu, K. W.; Tang, M. M. K.; Chen, M. J.; Guo, Z. F.; Guo, Z. H.; Coghi, P.; Monti, D. Reactions of Antimalarial Peroxides with Each of Leucomethylene Blue and Dihydroflavins: Flavin Reductase and the Cofactor Model Exemplified. *ChemMedChem* **2011**, *6*, 279–291.

(16) Vennerstrom, J. L.; Fu, H. N.; Ellis, W. Y.; Ager, A. L.; Wood, J. K.; Andersen, S. L.; Gerena, L.; Milhous, W. K. Dispiro-1,2,4,5-Tetraoxanes: A New Class of Antimalarial Peroxides. *J. Med. Chem.* **1992**, *35*, 3023–3027.

(17) Amewu, R.; Stachulski, A. V.; Ward, S. A.; Berry, N. G.; Bray, P. G.; Davies, J.; Labat, G.; Vivas, L.; O'Neill, P. M. Design and Synthesis of Orally Active Dispiro 1,2,4,5-Tetraoxanes; Synthetic Antimalarials with Superior Activity to Artemisinin. *Org. Biomol. Chem.* **2006**, *4*, 4431–4436.

(18) Ellis, G. L.; Amewu, R.; Sabbani, S.; Stocks, P. A.; Shone, A.; Stanford, D.; Gibbons, P.; Davies, J.; Vivas, L.; Charnaud, S.; Bongard, E.; Hall, C.; Rimmer, K.; Lozanom, S.; Jesus, M.; Gargallo, D.; Ward, S. A.; O'Neill, P. M. Two-Step Synthesis of Achiral Dispiro-1,2,4,5-Tetraoxanes with Outstanding Antimalarial Activity, Low Toxicity, and High-Stability Profiles. *J. Med. Chem.* **2008**, *51*, 2170–2177.

(19) O'Neill, P. M.; Amewu, R. K.; Nixon, G. L.; Bousejra-El Garah, F.; Mungthin, M.; Chadwick, J.; Shone, A. E.; Vivas, L.; Lander, H.; Barton, V.; Muangnoicharoen, S.; Bray, P. G.; Davies, J.; Park, B. K.; Wittlin, S.; Brun, R.; Preschel, M.; Zhang, K. S.; Ward, S. A. Identification of a 1,2,4,5-Tetraoxane Antimalarial Drug-Development Candidate (RKA 182) with Superior Properties to the Semisynthetic Artemisinins. *Angew. Chem., Int. Ed.* **2010**, *49*, 5693–5697.

(20) Kumura, N.; Furukawa, H.; Onyango, A. N.; Izumi, M.; Nakajima, S.; Ito, H.; Hatano, T.; Kim, H. S.; Wataya, Y.; Baba, N. Different Behavior of Artemisinin and Tetraoxane in the Oxidative Degradation of Phospholipid. *Chem. Phys. Lipids* **2009**, *160*, 114–120.

(21) Jackson, K. E.; Klonis, N.; Ferguson, D. J. P.; Adisa, A.; Dogovski, C.; Tilley, L. Food Vacuole-Associated Lipid Bodies and Heterogeneous Lipid Environments in the Malaria Parasite, *Plasmodium falciparum*. *Mol. Microbiol.* **2004**, *54*, 109–122.

(22) Charman, S. A.; Arbe-Barnes, S.; Bathurst, I. C.; Brun, R.; Campbell, M.; Charman, W. N.; Chiu, F. C. K.; Chollet, J.; Craft, J. C.; Creek, D. J.; Dong, Y.; Matile, H.; Maurer, M.; Morizzi, J.; Nguyen, T.; Papastogiannidis, P.; Scheurer, C.; Shackleford, D. M.; Sriraghavan, K.; Stingelin, L.; Tang, Y.; Urwyler, H.; Wang, X.; White, K. L.; Wittlin, S.; Zhou, L.; Vennerstrom, J. L. Synthetic Ozonide Drug Candidate OZ439 Offers New Hope for a Single-Dose Cure of Uncomplicated Malaria. *Proc. Natl. Acad. Sci. U.S.A.* **2011**, *108*, 4400–4405.

(23) Opsenica, I.; Terzic, N.; Opsenica, D.; Angelovski, G.; Lehnig, M.; Eilbracht, P.; Tinant, B.; Juranic, Z.; Smith, K. S.; Yang, Y. S.; Diaz, D. S.; Smith, P. L.; Milhous, W. K.; Dokovic, D.; Solaja, B. A. Tetraoxane Antimalarials and Their Reaction with Fe(II). *J. Med. Chem.* **2006**, *49*, 3790–3799.

(24) Tang, Y. Q.; Dong, Y. X.; Wang, X. F.; Sriraghavan, K.; Wood, J. K.; Vennerstrom, J. L. Dispiro-1,2,4-trioxane Analogues of a Prototype Dispiro-1,2,4-trioxolane: Mechanistic Comparators for Artemisinin in the Context of Reaction Pathways with Iron(II). *J. Org. Chem.* **2005**, *70*, 5103–5110.

(25) Haynes, R. K.; Ho, W. Y.; Chan, H. W.; Fugmann, B.; Stetter, J.; Croft, S. L.; Vivas, L.; Peters, W.; Robinson, B. L. Highly Antimalaria-Active Artemisinin Derivatives: Biological Activity Does Not Correlate with Chemical Reactivity. *Angew. Chem., Int. Ed.* **2004**, *43*, 1381–1385.

(26) Spiteller, G. Linoleic Acid Peroxidation, the Dominant Lipid Peroxidation Process in Low Density Lipoprotein, and Its Relationship to Chronic Diseases. *Chem. Phys. Lipids* **1998**, *95*, 105–162.

(27) Domingues, M. R. M.; Reis, A.; Domingues, P. Mass Spectrometry Analysis of Oxidized Phospholipids. *Chem. Phys. Lipids* **2008**, *156*, 1–12.

(28) Reis, A.; Domingues, P.; Ferrer-Correia, A. J. V.; Domingues, M. R. M. Fragmentation Study of Short-Chain Products Derived from Oxidation of Diacylphosphatidylcholines by Electrospray Tandem Mass Spectrometry: Identification of Novel Short-Chain Products. *Rapid Commun. Mass Spectrom.* **2004**, *18*, 2849–2858.

(29) Berman, P. A.; Adams, P. A. Artemisinin Enhances Heme-Catalysed Oxidation of Lipid Membranes. *Free Radical Biol. Med.* **1997**, *22*, 1283–1288.

(30) Bousejra-El Garah, F.; Meunier, B.; Robert, A. The Antimalarial Artemisone Is an Efficient Heme Alkylating Agent. *Eur. J. Inorg. Chem.* **2008**, 2133–2135.

(31) Creek, D. J.; Charman, W. N.; Chiu, F. C. K.; Prankerd, R. J.; Dong, Y.; Vennerstrom, J. L.; Charman, S. A. Relationship between Antimalarial Activity and Heme Alkylation for Spiro- and Dispiro-1,2,4-Trioxolane Antimalarials. *Antimicrob. Agents Chemother.* **2008**, *52*, 1291–1296.

(32) Laurent, S. A. L.; Loup, C.; Mourgues, S.; Robert, A.; Meunier, B. Heme Alkylation by Artesunic Acid and Trioxaquine DU1301, Two Antimalarial Trioxanes. *ChemBioChem* **2005**, *6*, 653–658.

(33) Robert, A.; Coppel, Y.; Meunier, B. NMR Characterization of Covalent Adducts Obtained by Alkylation of Heme with the Antimalarial Drug Artemisinin. *Inorg. Chim. Acta* **2002**, *339*, 488–496.

(34) Yields of adducts were estimated by measuring their concentration by LC-MS.

(35) Robert, A.; Meunier, B. Characterization of the First Covalent Adduct between Artemisinin and a Heme Model. *J. Am. Chem. Soc.* **1997**, *119*, 5968–5969.

(36) Huey, R.; Morris, G. M.; Olson, A. J.; Goodsell, D. S. A Semiempirical Free Energy Force Field with Charge-Based Desolvation. *J. Comput. Chem.* **2007**, *28*, 1145–1152.

(37) Vennerstrom, J. L.; Dong, Y.; Chollet, J.; Matile, H. Preparation of Spiro/Dispiro-1,2,4-Trioxolanes As Antimalarial Agents. US6486-199B1, 2002.

(38) Frisch, M. J.; Trucks, G. W.; Schlegel, H. B.; Scuseria, G. E.; Robb, M. A.; Cheeseman, J. R.; Montgomery, J., J. A.; Vreven, T.; Kudin, K. N.; Burant, J. C.; Millam, J. M.; Iyengar, S. S.; Tomasi, J.; Barone, V.; Mennucci, B.; Cossi, M.; Scalmani, G.; Rega, N.; Petersson, G. A.; Nakatsuji, H.; Hada, M.; Ehara, M.; Toyota, K.; Fukuda, R.; Hasegawa, J.; Ishida, M.; Nakajima, T.; Honda, Y.; Kitao, O.; Nakai, H.; Klene, M.; Li, X.; Knox, J. E.; Hratchian, H. P.; Cross, J. B.; Bakken, V.; Adamo, C.; Jaramillo, J.; Gomperts, R.; Stratmann, R. E.; Yazyev, O.; Austin, A. J.; Cammi, R.; Pomelli, C.; Ochterski, J. W.; Ayala, P. Y.; Morokuma, K.; Voth, G. A.; Salvador, P.; Dannenberg, J. J.; Zakrzewski, V. G.; Dapprich, S.; Daniels, A. D.; Strain, M. C.; Farkas, O.; Malick, D. K.; Rabuck, A. D.; Raghavachari, K.; Foresman, J. B.; Ortiz, J. V.; Cui, Q.; Baboul, A. G.; Clifford, S.; Cioslowski, J.; Stefanov, B. B.; Liu, G.; Liashenko, A.; Piskorz, P.; Komaromi, I.; Martin, R. L.; Fox, D. J.; Keith, T.; Al-Laham, M. A.; Peng, C. Y.; Nanayakkara, A.; Challacombe, M.; Gill, P. M. W.; Johnson, B.; Chen, W.; Wong, M. W.; Gonzalez, C.; Pople, J. A. *Gaussian 03*, revision C.02; Gaussian, Inc.: Wallingford CT, 2004.